

SPIDER Calibration Techniques

CMB-Cal Workshop
University Milan at Bicocca, Italy
4 Nov 2024

Elle Shaw on behalf of the SPIDER Collaboration
University of Texas at Austin

Outline

1. SPIDER Project Overview

2. Pre-Flight Calibration



3. In-Flight Measurements



4. Post-Flight Analysis



SPIDER Collaboration

Two flights and lots of people

~ 80 members

~ 30 institutions

This talk covers:

SPIDER-1 Calibration discussed in B-mode
constraint paper (2022)

<https://doi.org/10.3847/1538-4357/ac20df>

Ongoing work with SPIDER-2 data analysis



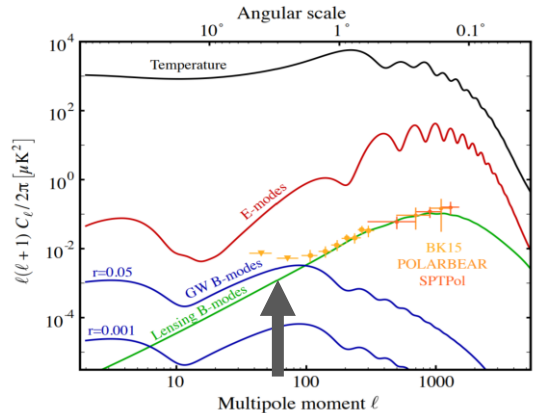
Spider 1 Deployment Team
2015



Spider 2 Deployment Team
2022

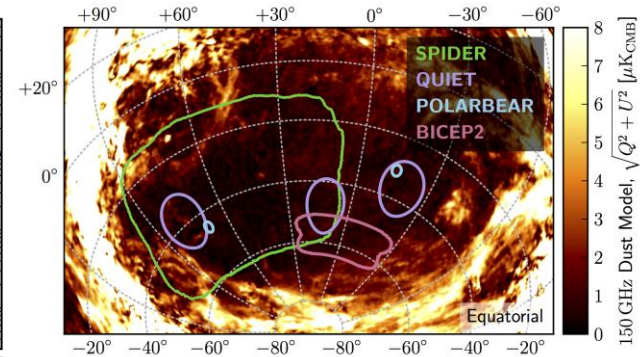
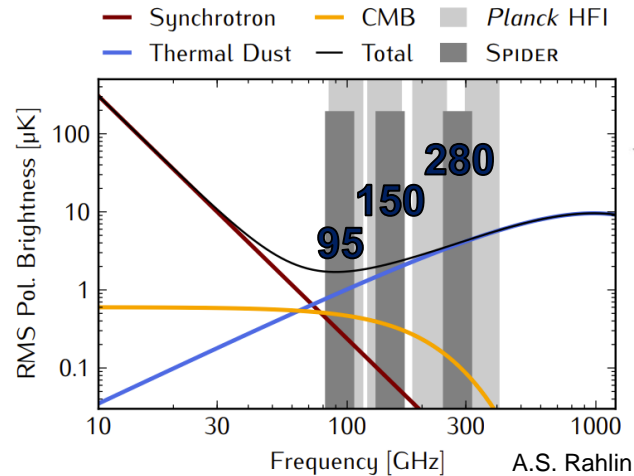
The SPIDER Program

Target: Faint B-mode polarization in the CMB at degree angular scales. $r \leq 0.03$



SPIDER's science goals are to:

- Measure peak amplitude of the CMB B-mode angular power spectrum at **degree scales**
- Verify **frequency spectrum** and produce the best signal-to-noise maps of **polarized Galactic dust foregrounds**
- Verify statistical isotropy of the signal by covering a **large sky area**.



Ballooning Platform Advantage

Balloon Opportunity:

- Limited atmospheric emission:
 - Keep sensitivity to large-scale modes with out the variability of atmosphere.
 - Reclaim access to high frequencies that are obscured from the ground.
 - Detector sensitivity - ability to approach CMB photon noise limit
- Make sensitive maps in less time



Ballooning Platform Advantage



Balloon Opportunity:

- Limited atmospheric emission:
 - Keep sensitivity to large-scale modes with out the variability of atmosphere.
 - Reclaim access to high frequencies that are obscured from the ground.
 - Detector sensitivity - ability to approach CMB photon noise limit
- Make sensitive maps in less time

Balloon Challenges (from calibration viewpoint):

- Short flights, unpredictable length
- Limited availability of astrophysical sources/time allocation
- Limited real-time feedback on instrument status
- COVID + Antarctica == rushed launch and deployment schedule

First Flight 2015

- January 1-18, 2015
- All critical payload systems were operational!
- Science analysis $33 \leq l \leq 257$
- (95 GHz, 150 GHz)

Publications

[SPIDER Collab. ApJ \(2024\)](#) - Foregrounds: polarized dust emission

[Filippini et al JLTP \(2022\)](#) - In-flight gain monitoring

[Leung et al 2022 ApJ 928 109](#) - Simulation-based mode coupling correction

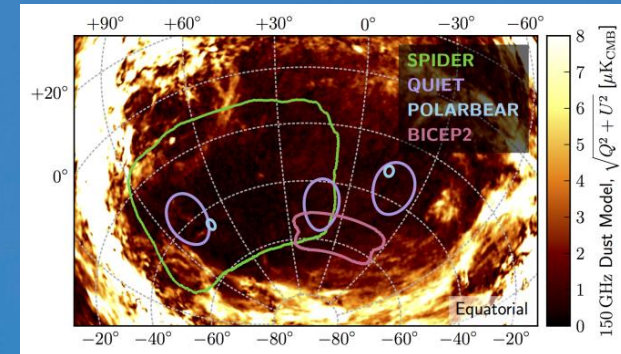
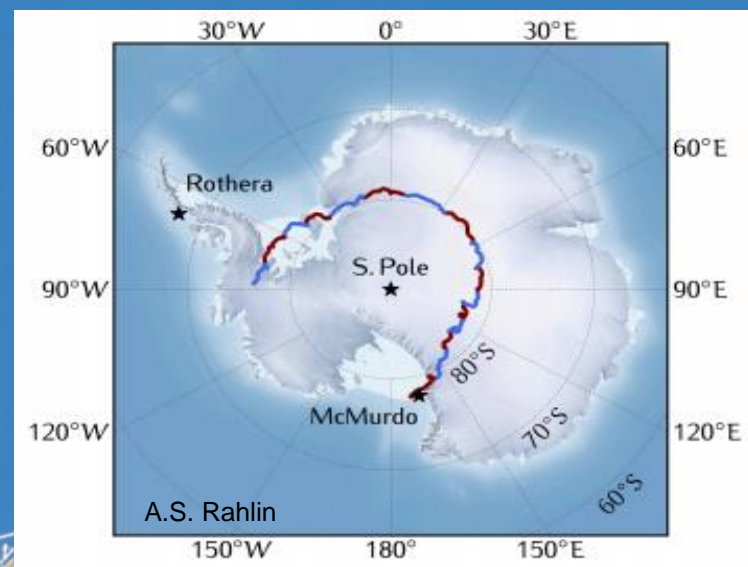
[SPIDER Collab. 2022 ApJ 927 174](#) - Spider-1 B-mode constraint

[Gambrel et al 2021 ApJ 922 132](#) - XFaster power spectrum and likelihood estimator

[Osherson et al JLTP \(2020\)](#) - Cosmic ray study on antenna-coupled TESs

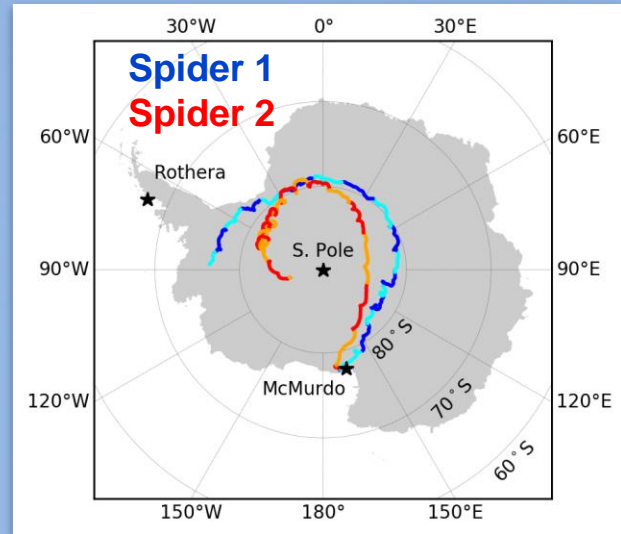
[Gualtieri et al JLTP \(2018\)](#) - First flight performance review

[Nagy et al ApJ 844 151 \(2017\)](#) - Upper limit on circular polarization

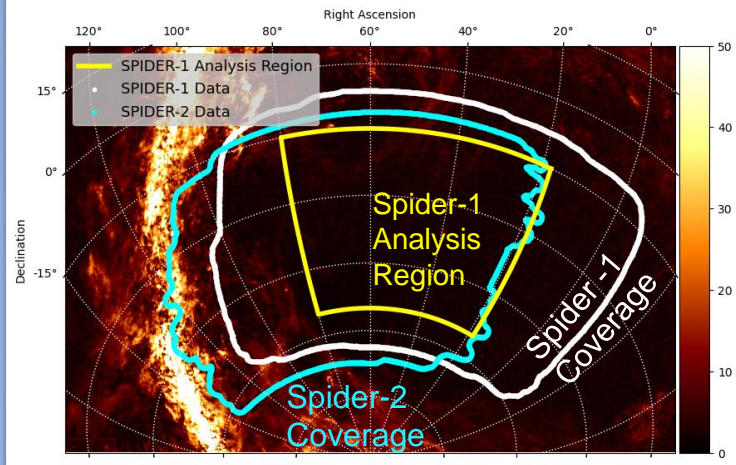


Second Flight 2022

- December 22, 2022 – January 7, 2023
- 95 GHz, 150 GHz, 280 GHz
- Pointing, power, thermal management, HWP, and communications systems **all good**
- No star cameras
- CMB observations through day 9



SPIDER 1+2 with Commander Polarized Dust



Publications:

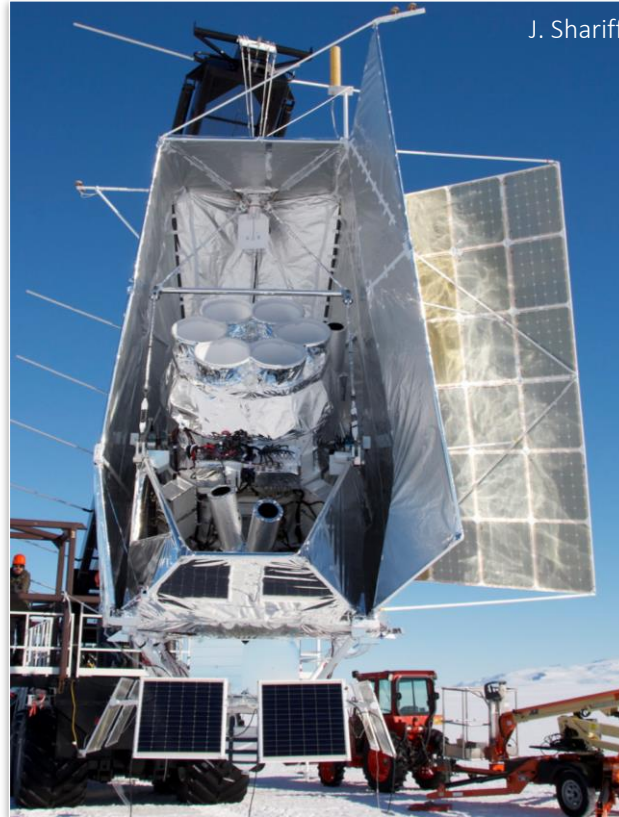
[Shaw *et al.* JATIS \(2024\) \(in review\)](#)
In-flight Performance of Spider's 280 GHz receivers.

The SPIDER Payloads

- ~2000 detectors
- ~1300 L liquid helium cryostat
- Lightweight carbon fiber and aluminum gondola
- Mylar sunshield
- Solar powered
- Pointing controlled by pivot motor and reaction wheel.
- Star cameras to reconstruct pointing

SPIDER-1

January 2015



J. Shariff

(3 x 95 GHz, 3 x 150 GHz)

SPIDER-2 Dec. 2022 – Jan. 2023

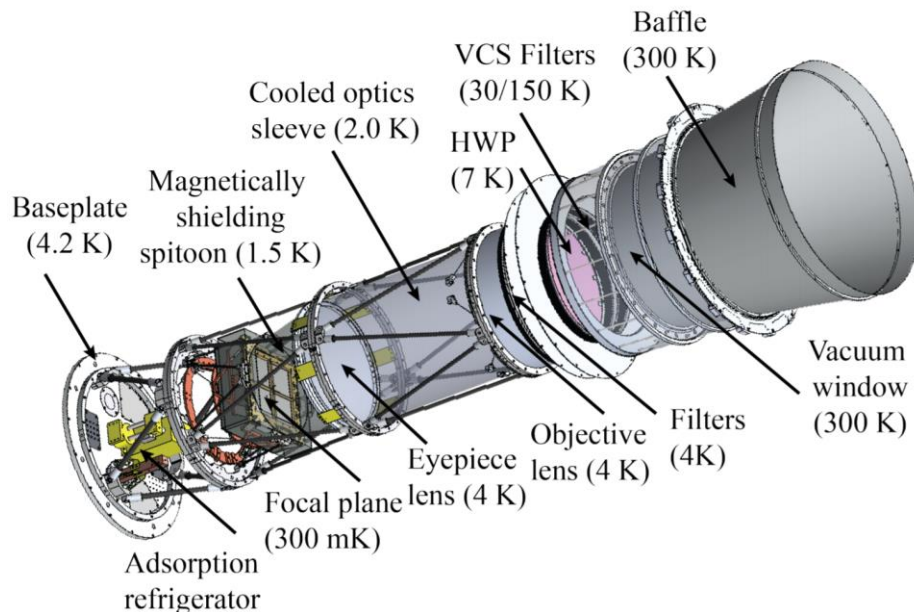


E. Shaw

(2 x 95 GHz, 1 x 150 GHz, 3 x 280 GHz)

SPIDER Receivers

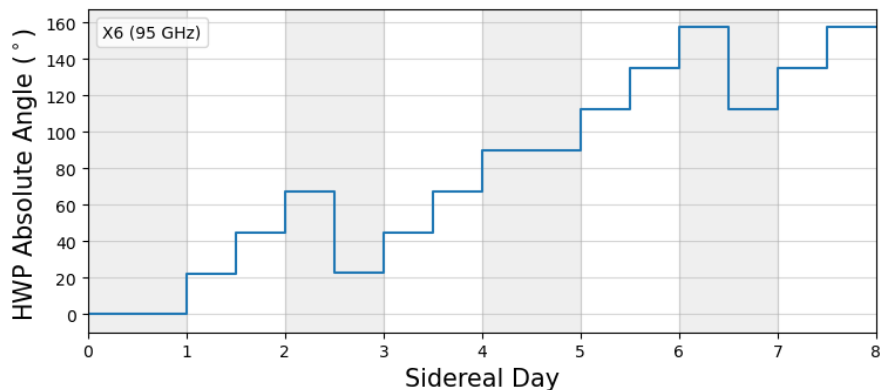
- 6 on-axis monochromatic refractors
- Stepped Half Wave Plates
- Emphasis on **low internal loading**
 - *Thin vacuum window –*
3.2 mm (95, 150) 1.6 mm (280)
 - *Reflective filter stack*
 - *4K Cooled Optics*
 - *2K Optical baffling +*
Magnetic Shielding
 - *300 mK Focal Plane Units (FPUs)*
- SQUID multiplexed detector readout.



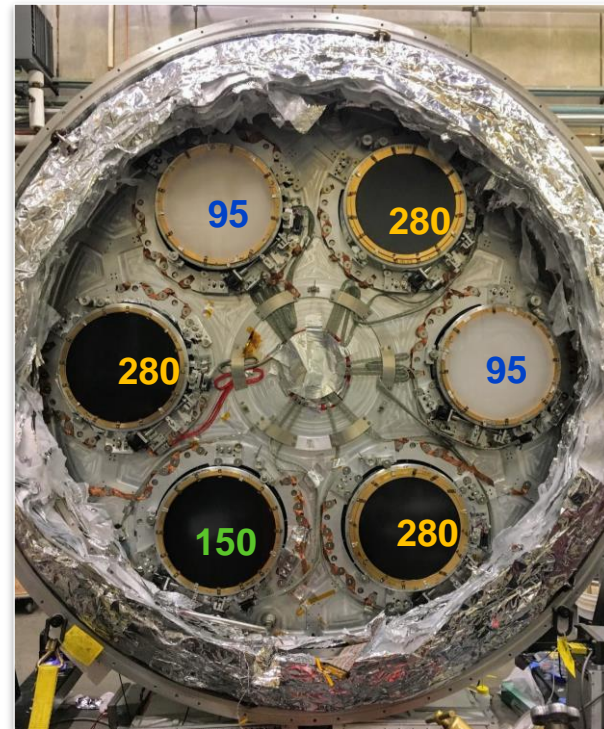
(90/150 GHz Receiver Diagram)
J. Gudmundsson

Half Wave Plates

- Polarization modulation with stepped Sapphire HWPs.
- AR Coating: Quartz (90 GHz), Cirlex (150, 280 GHz)
- Mounted to the top of the main helium tank above receiver apertures. (~ 7 K)
- Custom absolute and relative encoders reconstruct HWP angle to < 0.1 deg.



HWPs modulate the sky signal, reduce the effect of beam asymmetries and polarized instrumental systematics.



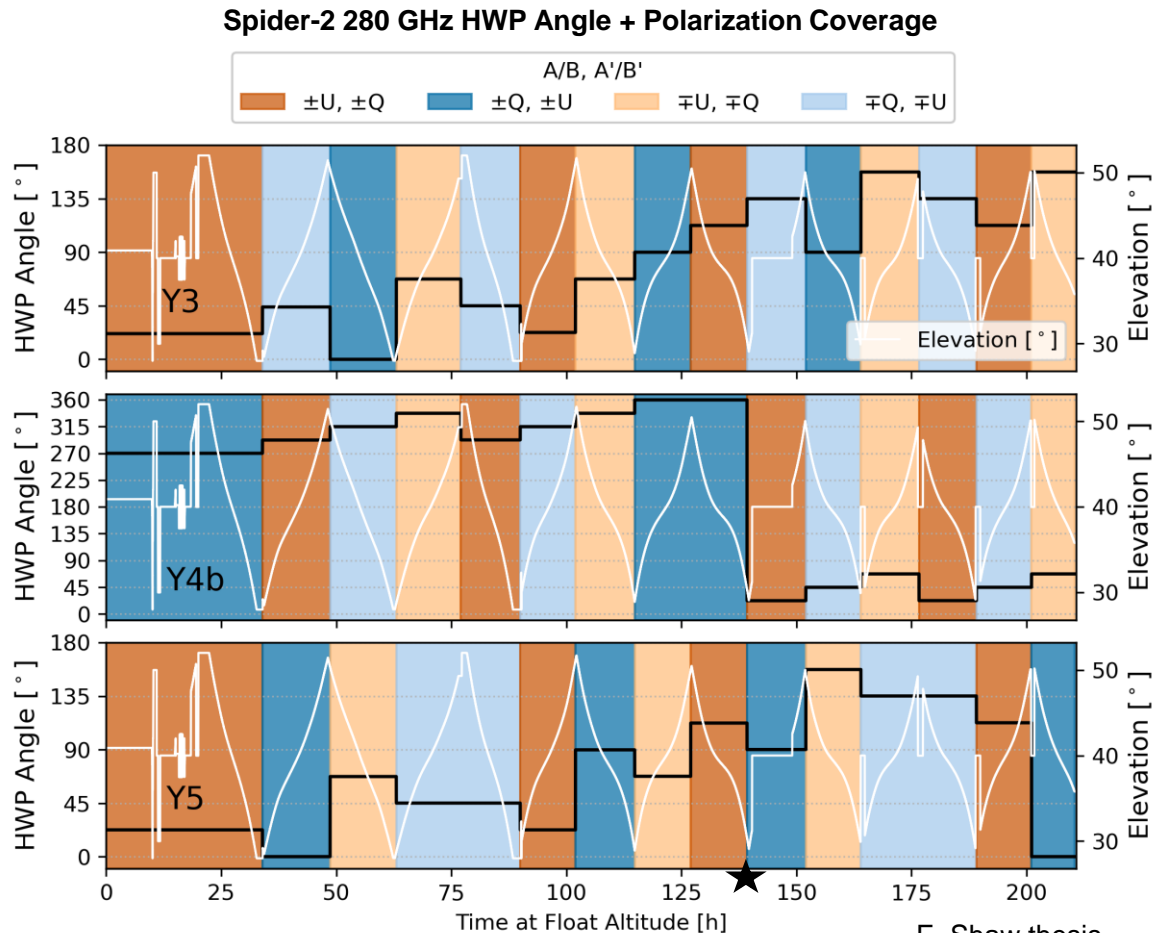
Spider-2 HWPs

HWP Rotation

HWPs rotate in multiples of 22.5° twice per sidereal day.

The schedule is optimized first to allow all detectors to cover $\pm Q$, $\pm U$ with an up and down scan (8 steps in 4 days)

Then, the schedule repeats at $+90^\circ$ to address HWP non-idealities if flight length allows.

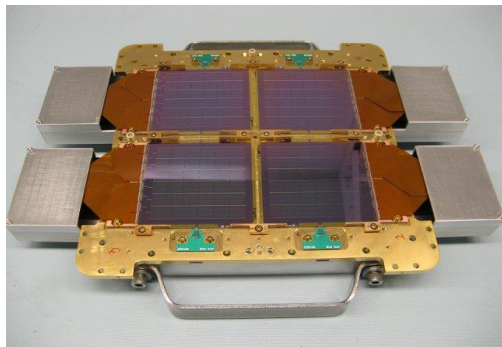


E. Shaw thesis

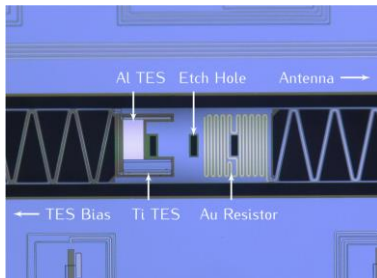
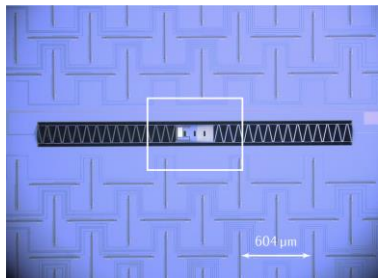
SPIDER Detector Technology

95 & 150 GHz

Slot antenna-coupled TES bolometer arrays
(JPL). Four tiles per focal plane unit (FPU).



[Ade et al. ApJ \(2015\)](#)



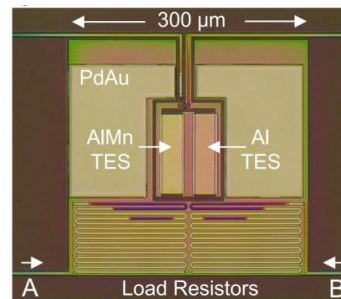
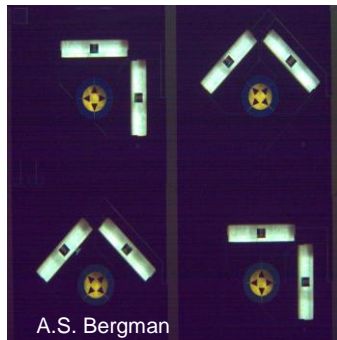
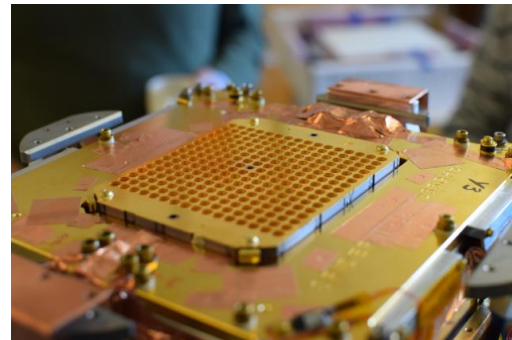
BOTH:

Dual TES design.

High-Tc transition for in-lab
characterization.

280 GHz

512 feedhorn-OMT coupled TESs
(NIST). Alternating pixel orientation.



Hubmayr et al. Proc SPIE
1606.09396

Calibration Tests

Pre-Flight

- Beam Mapping
- Fourier Transform Spectroscopy
- Detector Polarization Angle *

(*) Used directly in mapmaking

During Flight

- RCW 38 observations (Spider-1 Only)
- Bias Steps – monitor bias and relative gain

Post-Flight Analysis

- Absolute Pointing
- Absolute Calibration
- Beams Characterization

... Using iterative cross-calibration with external data sets.

Further checks on systematics:

Simulations of Systematics

Data Split Null Tests

Systematics error budget designed to meet requirements for $r < 0.03$ at $\ell = 100$

Pre-Flight Calibration Measurements



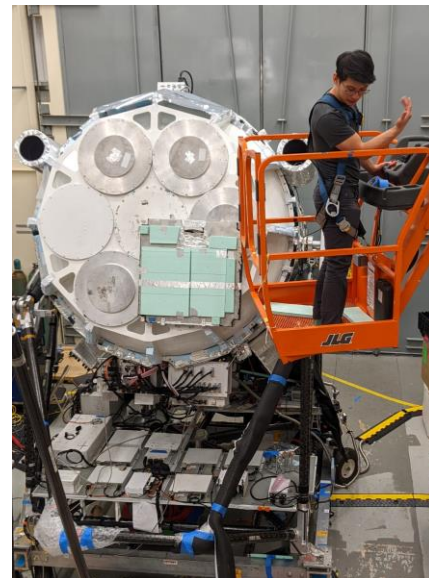
Optical Efficiency

Room temperature & liquid nitrogen source used to measure detector responsivity.

Used alongside I-V curves acquired during flight to make preliminary absolute calibration estimates. ([2408.10444](https://doi.org/10.2408.10444))

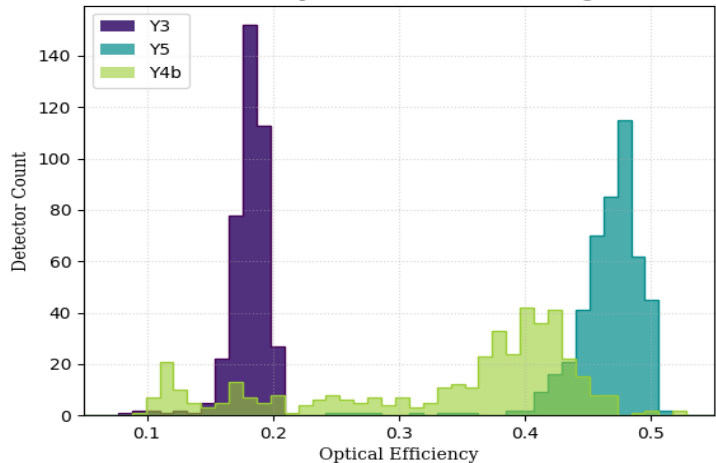


LN2 bucket for test cryostat.
Zotefoam bucket + HR-25 +
Aluminum Plate

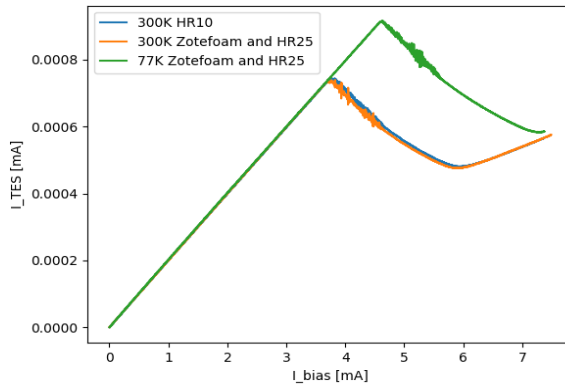


Tiltable LN2 bucket for flight cryostat.
J. Nagy.

280 GHz Optical Efficiencies as in Flight



r11c10 Al IV Curves



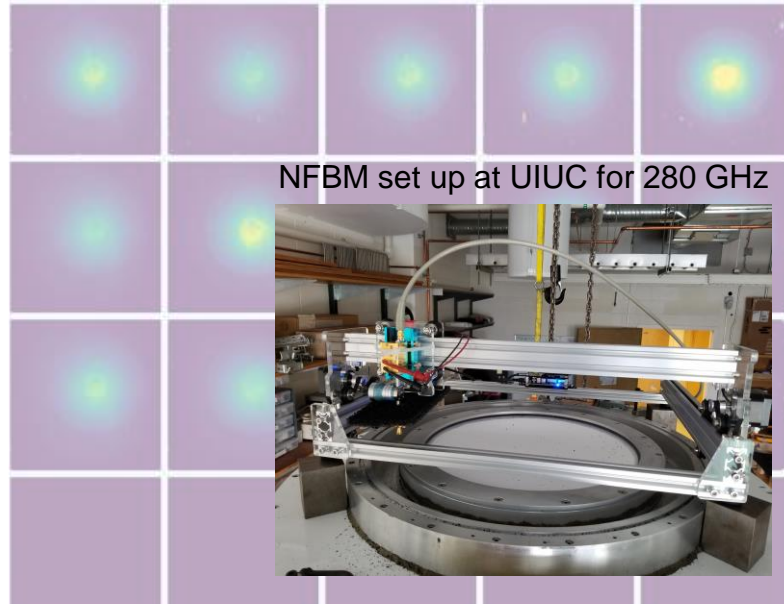
Near and Far-Field Beam Mapping

Beam mapping results are used for comparison to beam simulations for confirmation that the as-built optics matched the design.

Near-field beam mapping completed by both Spider-1 and Spider-2 using custom built scanning stages mounted at aperture of the test cryostat.

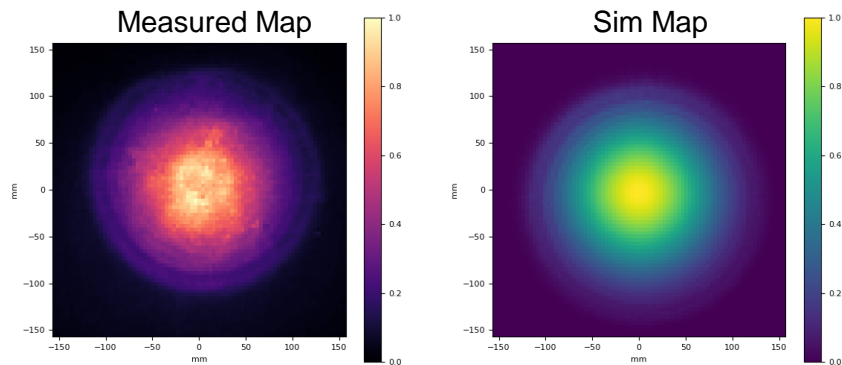
Far-field beam mapping was done for select 95 and 150 GHz focal planes during Spider-1 commissioning inside the Caltech high bay.

The far-field distance at 280 GHz proved logistically unfeasible.



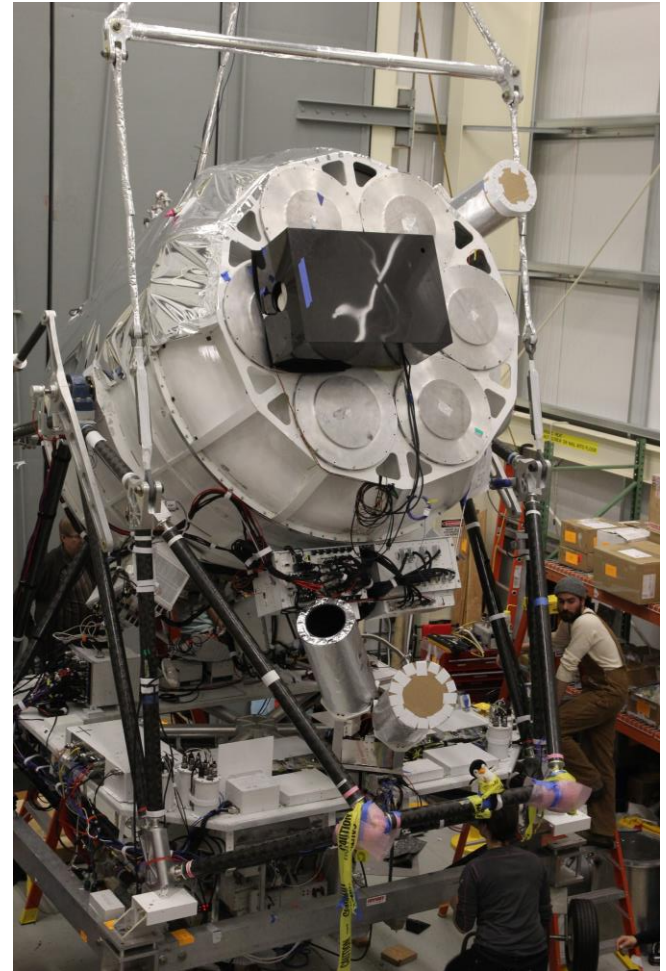
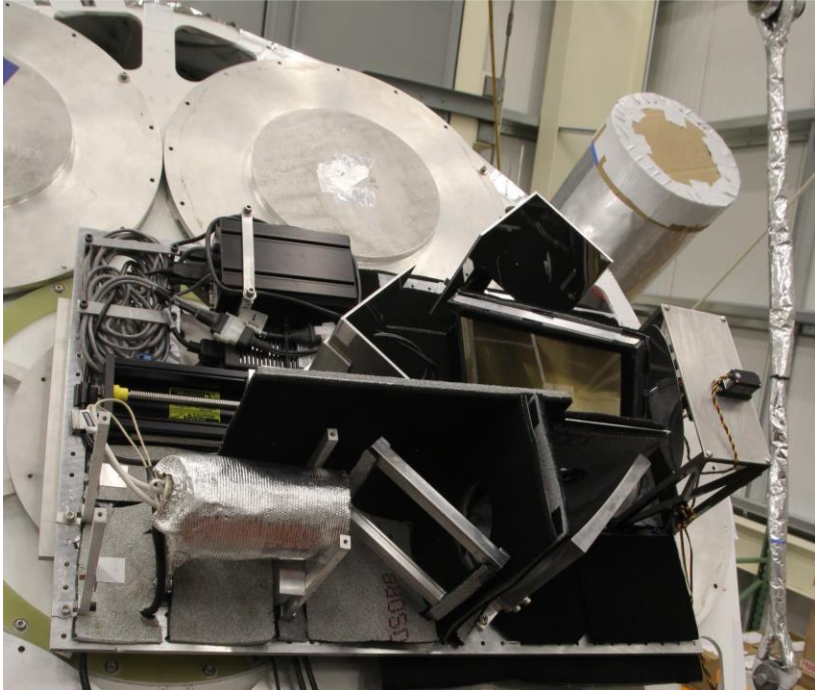
NFBM set up at UIUC for 280 GHz

Single detector comparison. 280 GHz.



Spectral Bandpass

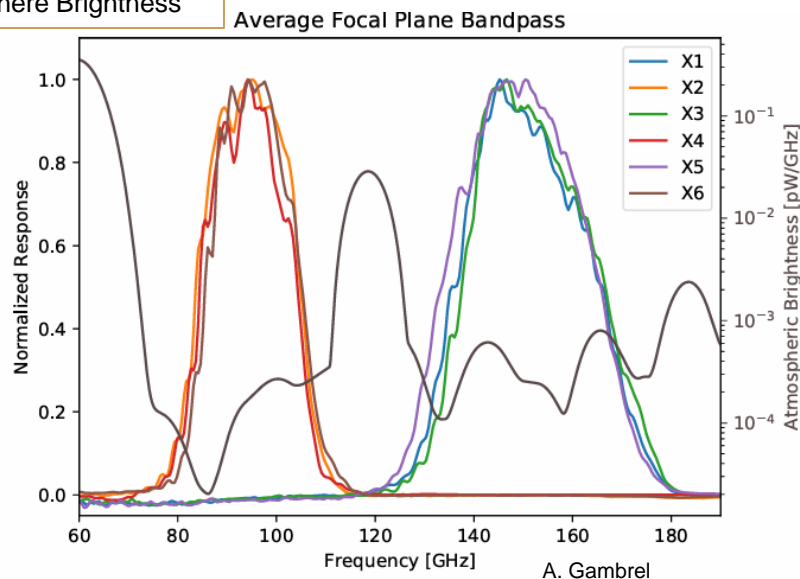
Custom Martin-Puplett Interferometer.
Lightweight, mountable to flight cryostat.



Spectral Bandpass

95% of all detectors used in science analysis for Spider-1 were measured with band center and width accurate to 1 GHz.

SPIDER-1 Band Pass +
Atmosphere Brightness



Per-detector measurements are *not* used directly in mapmaking. High/Low band center null tests show negligible leakage from bandpass mismatch in Spider-1 data.

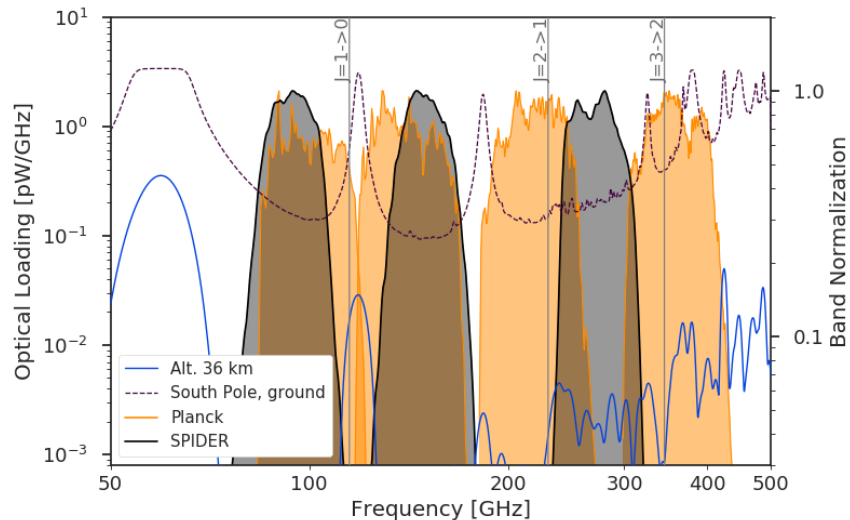
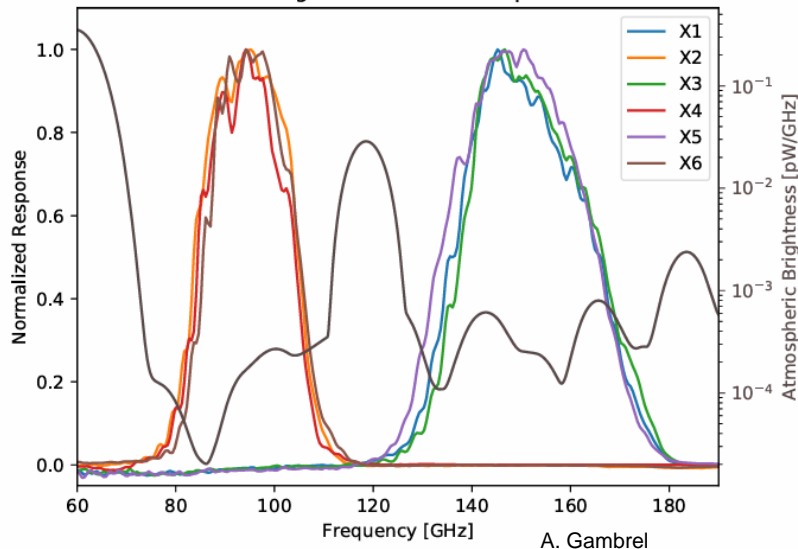
Spectral Bandpass

95% of all detectors used in science analysis for Spider-1 were measured with band center and width accurate to 1 GHz.

Similar measurements carried out prior to second flight, but only two of 280 GHz receivers characterized due to accelerated deployment and launch schedules.

SPIDER-1 Band Pass +
Atmosphere Brightness

Average Focal Plane Bandpass



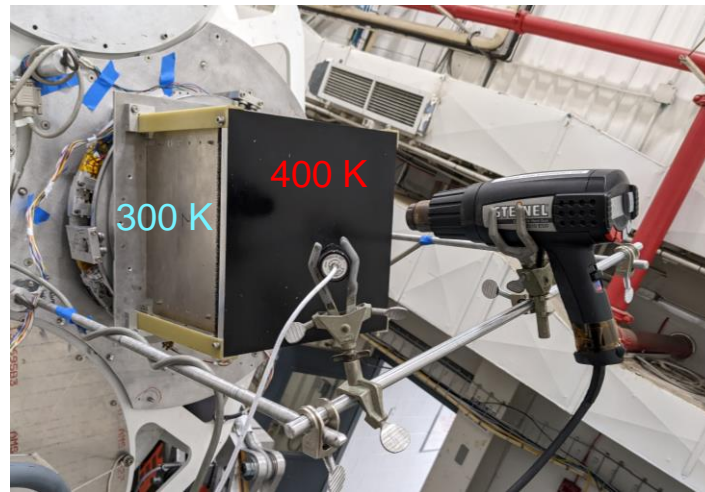
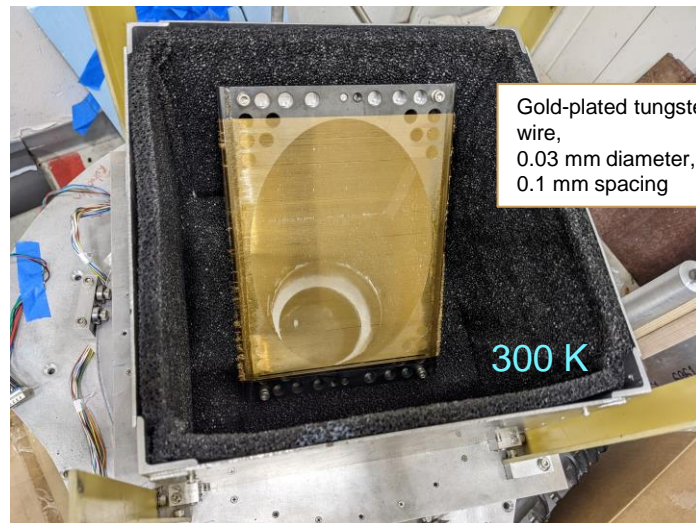
Detector Polarization Angle

Absolute and relative polarization angles, Ψ_{abs} , Ψ_{rel} , are measured before flight using a rotating polarized thermal source in the near field.

Apparatus:

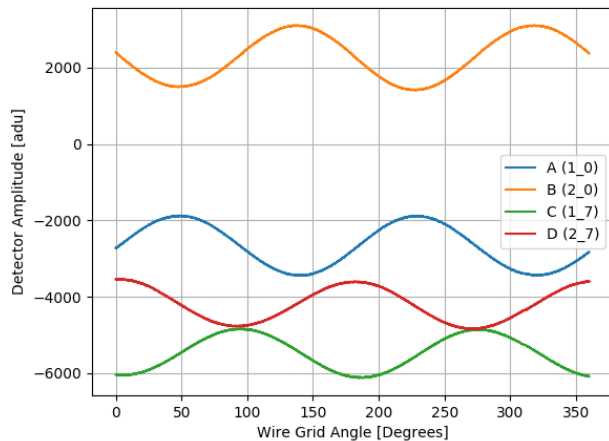
- Wire grid enclosed in HR-10 lined box.
- Lid of box is thermally isolated from sides and heated to ~ 400 K.
- Wiregrid + source box rotate on Spider prototype HWP rotation mechanism.

Target Sensitivity: 1° error on Ψ_{abs} , Ψ_{rel}
Achieved: $< 0.5^\circ$

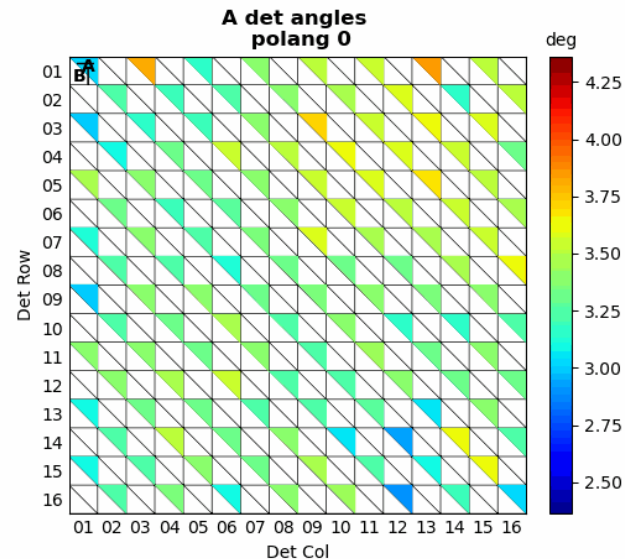


Detector Polarization Angle

- Relate min/max signals in data to wire grid rotation angle and HWP angles to determine detector angles.
- Rotate source + grid through ~ 3 turns, for all flight HWP angles (22.5 deg increments)
- Coverage of all HWP angles gives an estimate of non-ideality.



Data from four 280 GHz detectors, all four pol. angles represented.



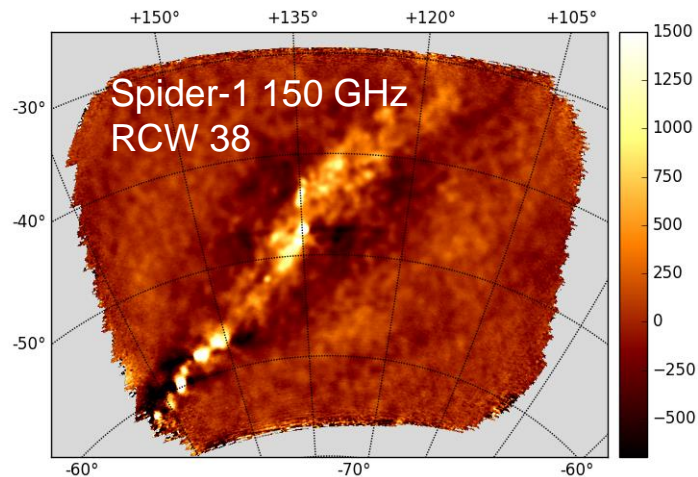
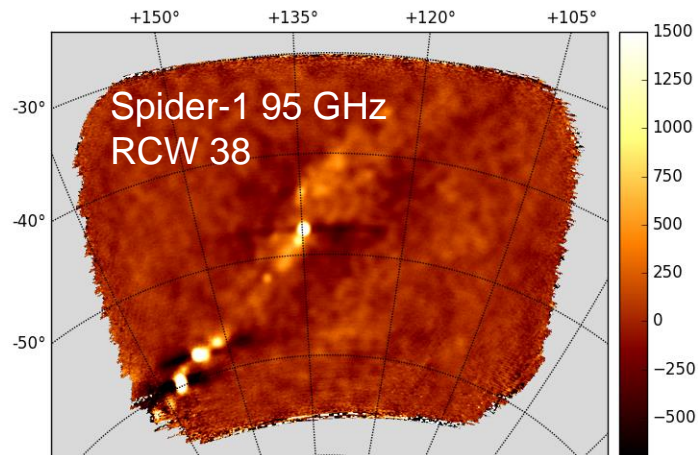
Measured detector angle relative to gravity, for A-type detectors on 280 GHz receiver, Y5, for multiple HWP rotation angles.

In-Flight Calibration Measurements



Astrophysical Sources

- Spider-1 devoted some flight time to observations of RCW 38 – massive star cluster in Galactic plane.
- Four ~70 minute scans.
- In the end low S/N too low to use for reliable absolute calibration.
- Used as a starting point for confirmation of pointing reconstruction and stability.
- Not scanned during Spider-2.



In-Flight Gain Monitoring

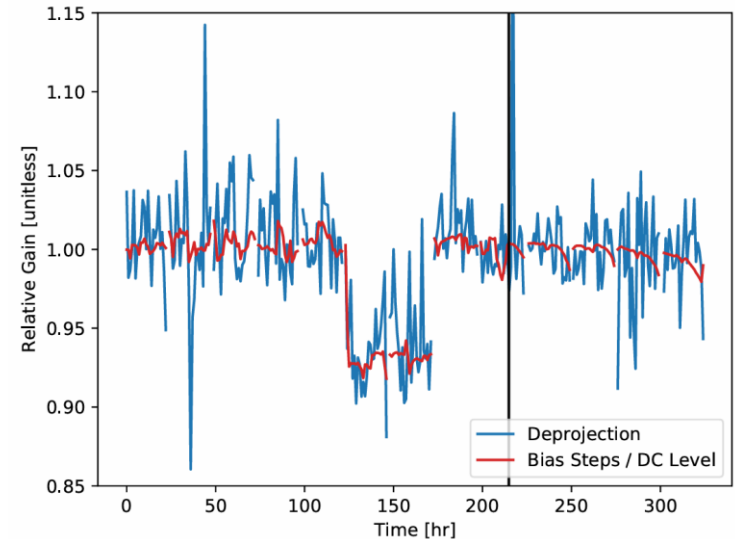
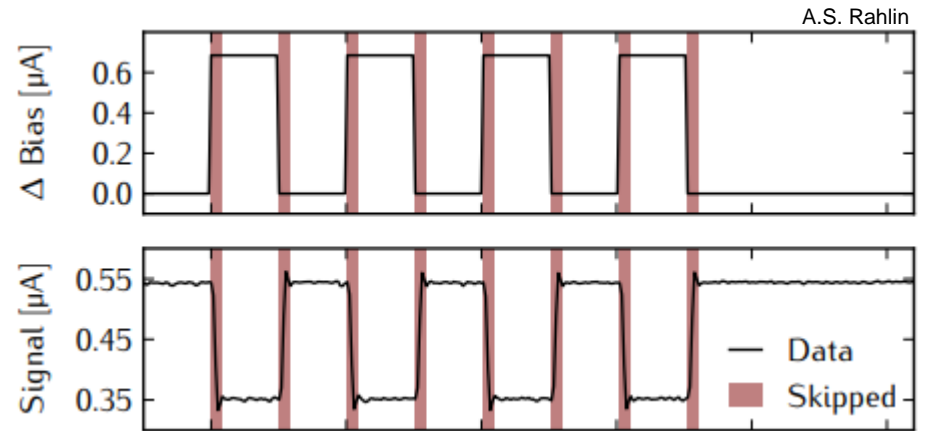
Gain variations on short time scales (~3 minutes) are monitored using bias steps.

Gain varies because of wafer temperatures, optical loading, and electrical bias.

Low-amplitude square wave injected into TES bias for 2 seconds @ 2 Hz, every 5 scan turnarounds, approximately every 3 minutes.

Used to create a relative correction to detector gain throughout flight... though was also shown to be unnecessary for Spider-1.

Automatically adjusts bias as necessary.



Post-Flight Calibration



Cross-Correlation with *Planck*

Absolute calibration (gain) and beam centroids are determined by minimizing a per-multipole residual with *Planck* temperature half-mission maps.

If the calibration and beams are accurate, then the ratio should be near to 1.

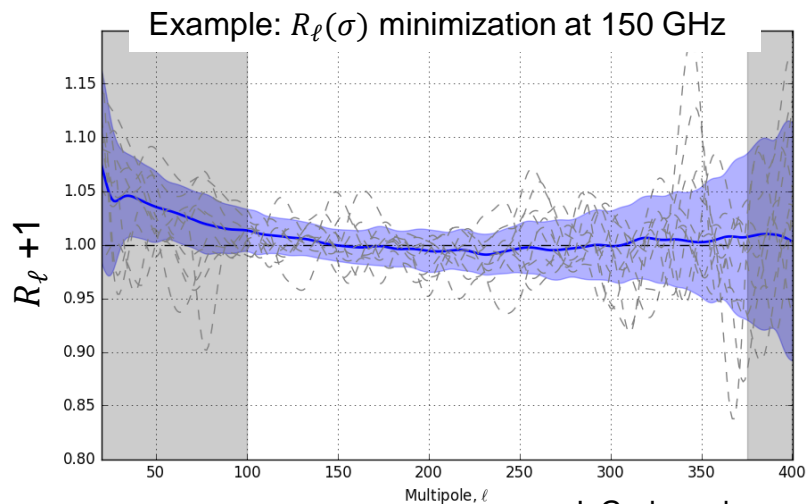
Minimize degree-scale power with *Planck* temperature anisotropy data at 100 and 143 GHz.

Ell min = 100

Ell max = 275 (95GHz), 375 (150 GHz)

$$\sum_{\ell=\ell_1}^{\ell_2} R_{\ell}(c, \sigma) \equiv \sum_{\ell=\ell_1}^{\ell_2} \left| c \frac{\hat{C}_{\ell}^{S \times P_2}}{\hat{C}_{\ell}^{P_1 \times P_2}} \frac{b_{\ell}^P}{b_{\ell}^S(\sigma)} - 1 \right|$$

Spider X *Planck* HM2
↑
HM1 x HM2
Beam window function



Absolute Calibration and Beams

2-Step Iterative Process

Start with baseline per-detector calibration product, **cal_1** and estimate of Spider beam, **beam_1**

1) Do per-FPU fits for the beam model

- 1a) Make per-FPU Spider maps using **cal_1**
- 1b) Reobserve *Planck* HM1 and HM2 using **beam_1**.
- 1c) Minimize R_ℓ with $\mathbf{c} = 1$ and fit for σ .

Make this the next per-FPU beam product, **beam_2**.

2) Do per-detector fits for absolute calibration

- 2a) Make Spider map for each detector.
- 2b) Reobserve *Planck* HM1 and HM2 using **beam_2**.
- 2c) Minimize R_ℓ , this time fit for \mathbf{c} for each detector.

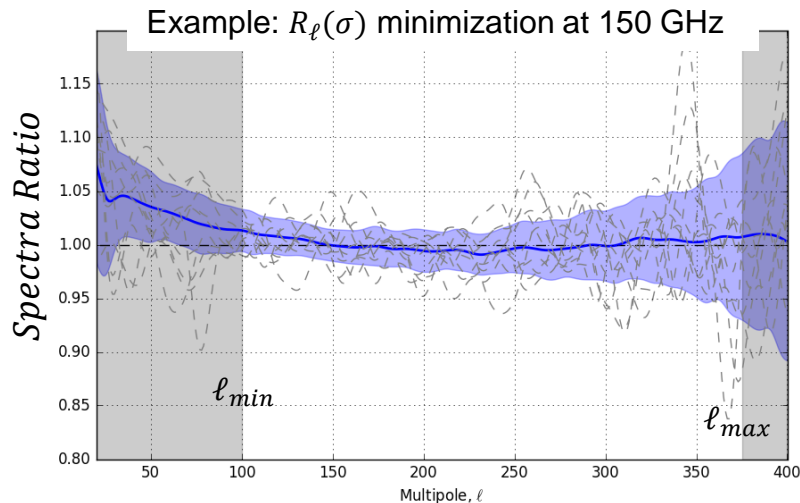
Make these \mathbf{c} 's into the next absolute calibration product, **cal_2**.

Repeat until it reaches convergence.

$$\sum_{\ell=\ell_{\min}}^{\ell_{\max}} R_\ell(\mathbf{c}, \sigma) \equiv \sum_{\ell_{\max}}^{\ell_{\min}} \left| \mathbf{c} \frac{\hat{C}_\ell^{S \times P_2}}{\hat{C}_\ell^{P_1 \times P_2}} \frac{b_\ell^P}{b_\ell^S(\sigma)} - 1 \right|$$

Spider X *Planck* HM2
↑
HM1 x HM2

Beam window function



Deprojection – Spider Implementation

Based on the “deprojection” technique developed by BICEP/Keck Array.

Analysis technique for constraining pointing offsets, beam parameters, and gain drifts.

Leaked polarization signal, $d_{\Theta \rightarrow P}$, described by the convolution of a difference beam with an unpolarized map Θ .

To second order, various *differential beam modes* couple to distinct linear combinations of Θ and its spatial derivatives.

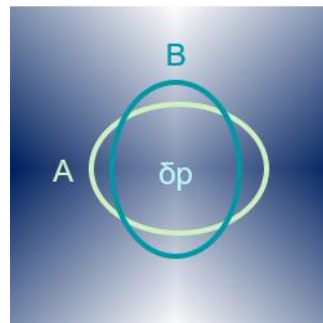
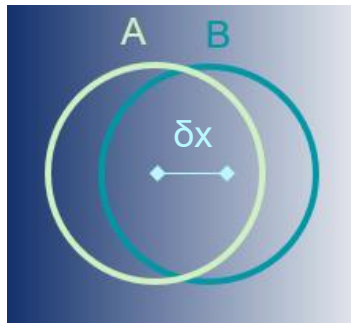
$$\begin{aligned} \text{e.g. } d_{\delta x}(t) &= \Theta * B_{\delta x}(\hat{p}(t)) \\ &= a_x \nabla_x \Theta * B(\hat{p}(t)) \end{aligned}$$

The beam abnormalities should be constant. So, the only variable in how the leaked signal would show up in data timestreams depends on how the detectors scanned across the map.

$$\begin{aligned} d_{\Theta \rightarrow P} &= \Theta * [B_A(\hat{p}) - B_B(\hat{p})] \\ &\equiv \Theta * B_{\delta}(\hat{p}) \end{aligned}$$

Modes of Diff. Elliptical Gaussian

- Differential gain (peak height) δg
- Differential pointing, (centroid offset) $(\delta x, \delta y)$
- Differential beam width $\delta \sigma$
- Differential ellipticity, $(\delta c, \delta p)$



References:

B2. III. Instrumental Systematics
ApJ **814** 110 (2015)

Ed Young Thesis (Princeton 2018)

Deprojection – Spider Implementation

1. Take spatial derivatives of *Planck* maps at reference frequency and smooth with Spider's best-fit circular-Gaussian beam.
2. Sample the maps along a detector's nominal pointing trajectory to construct leakage template timestreams, $d_{\delta k}(t)$.
3. Fit leakage templates to “self-differenced” Spider detector TODs, Δs . (Simulated timestream made with *Planck* data.)
4. Results in a fit coefficient for each beam mode.

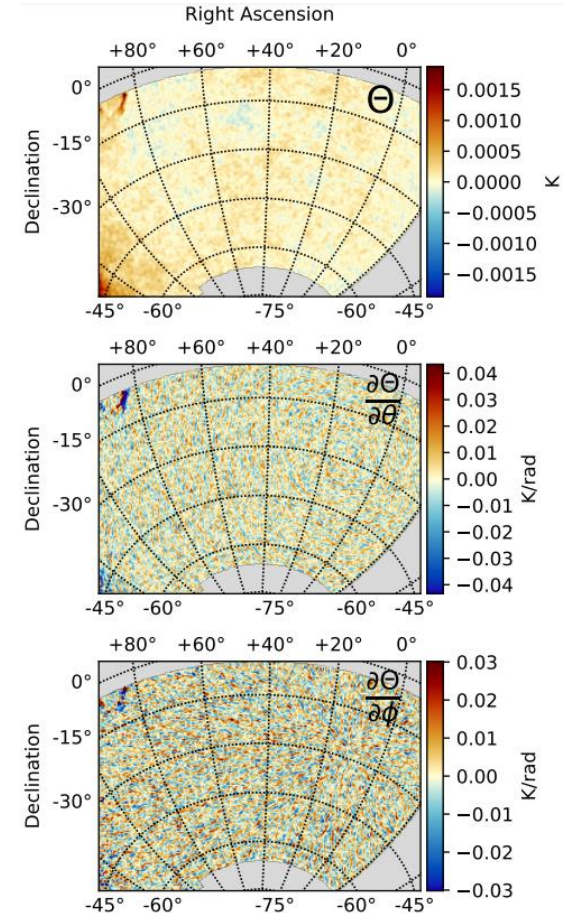
Modes of Diff. Elliptical Gaussian

- Differential gain (peak height) δg
- Differential pointing, (centroid offset) $(\delta x, \delta y)$
- Differential beam width $\delta \sigma$
- Differential ellipticity, $(\delta c, \delta p)$

Leakage template

$$d_{\delta}(t) = \sum_k a_k d_{\delta k}(t)$$

$$\Delta s = \det A - \det A_{sim}$$



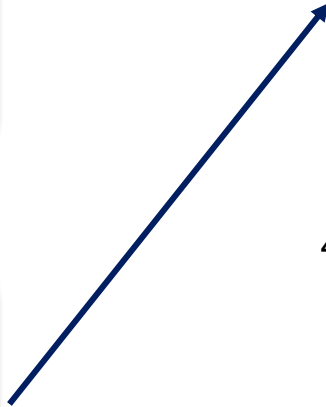
Pointing Reconstruction Spider-1

Boresight Pointing (time variant)

1. **In-flight Pointing Solution**
Uses on-board encoders and sensors (GPS, Magnetometer, Sun Sensors, Gyroscopes).
Error: 22'



2. **Integrated Pointing Solution**
Integrate between star camera solutions using gyroscope data.
Error: within 0.9' RMS of raw star camera solution.



Detector-Boresight Offsets (fixed)

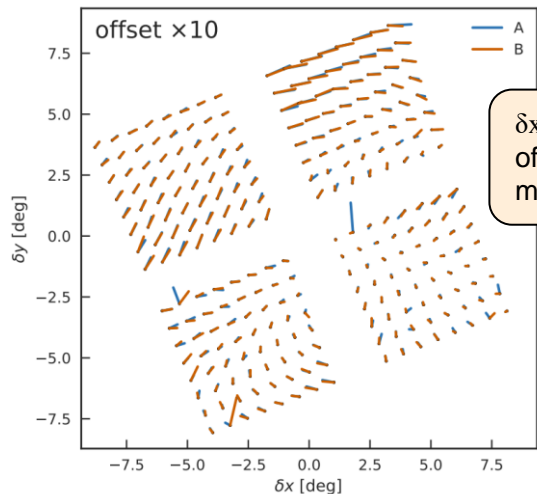
3. **Cross-correlation with *Planck* T maps**
Create initial plate-scale adjustments for each detector wafer, averaged for the full flight.



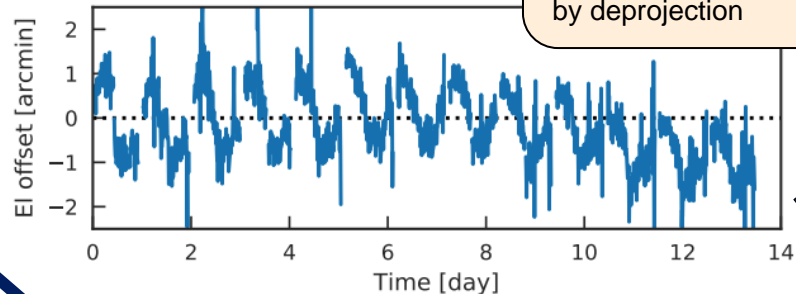
4. **Deprojection**

- Refine flight averaged per-detector offsets
- Refine boresight pointing solution with averages of detector offsets per 10 min chunk.

Deprojection gives most precise pointing and beam characterization



δx and δy offsets used in mapmaking.



Deprojection

- Refine flight averaged per-detector offsets.
- Refine boresight pointing solution with averages of detector offsets per 10 min chunk.

Target Beam Centroid Sensitivity: $\leq \sim 1.6'$
Achieved: $< 1'$; accurate to 0.8%

Pointing Reconstruction Spider-2

Boresight Pointing (time variant)

1.

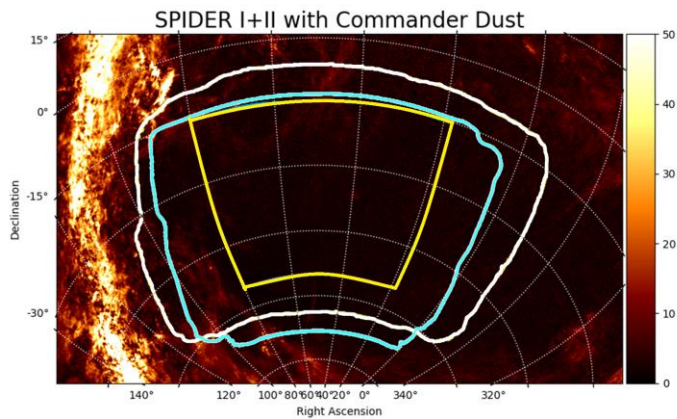
In-flight Pointing Solution

Uses on-board encoders and sensors (GPS, Magnetometers, Gyroscopes).

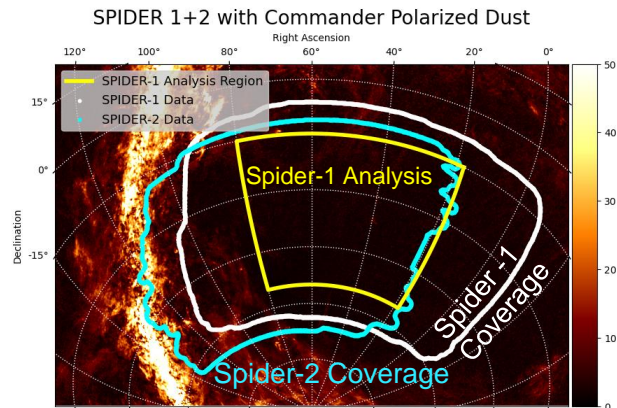


Pointing solution is still in development.

Relies on gyroscopes, elevation encoder, and inclinometer, and cross-correlations with *Planck*.



Best guess of sky coverage as of September 2023



Best estimate of sky coverage as of June 2024

Simulations + Null Tests

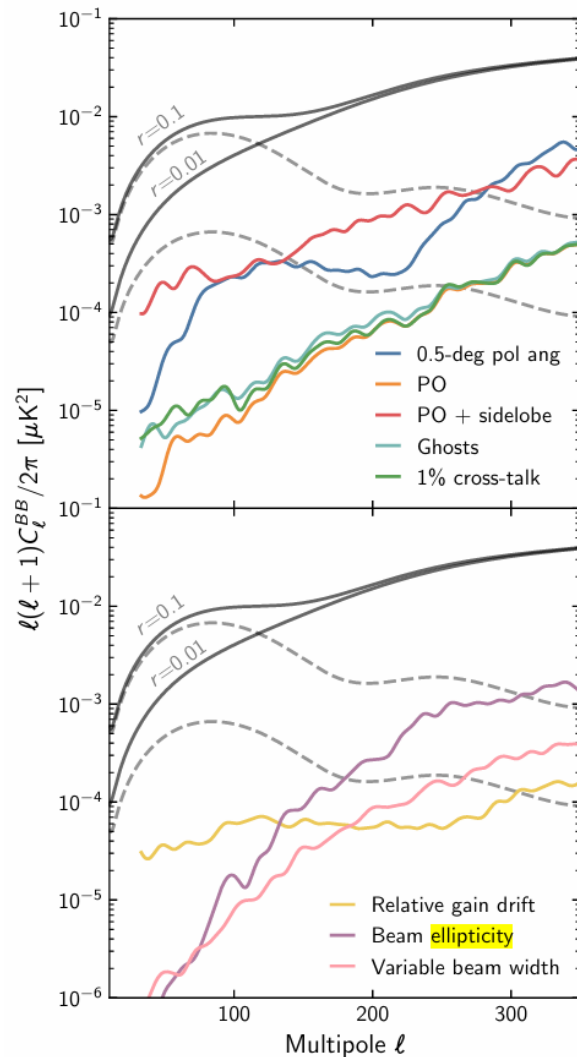
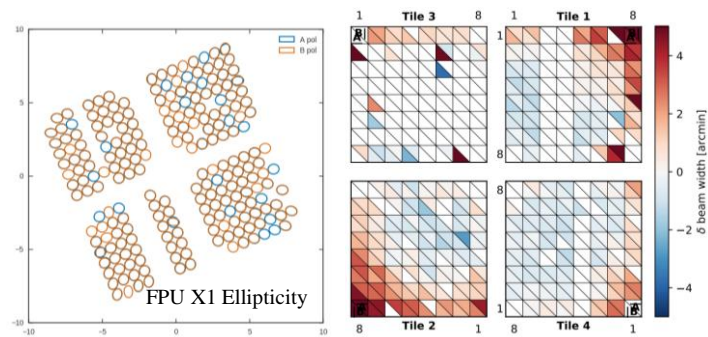
We verify that uncertainties in instrumental systematics from known and unknown sources won't affect scientific results.

Simulations look at :

- Beam non-Gaussianity, Ghosting, cross-talk, sidelobes (GRASP and *beamconv*)
- Polarization angle offsets, gain drift, beam ellipticity, variable beam widths. (Inputs are based on actual measurements or deprojection)

In all cases, no significant impact, on science results were found for Spider-1 data.

Differential beam width and ellipticity are fed into systematics sims.



Summary

The ballooning platform creates a unique opportunity to survey the CMB without the atmosphere in the way.

The observation time available with a balloon forces changes to calibration strategies.

SPIDER's approach can primarily rely on post-flight cross-correlations with external datasets to achieve absolute calibrations.

SPIDER-2 is in the thick of post-flight calibrations, using many of the same techniques as Spider-1



Thank you

SPIDER is supported in the U.S. by the National Aeronautics and Space Administration under grants NNX07AL64G, NNX12AE95G, and NNX17AC55G, 80NSSC21K1986 issued through the Science Mission Directorate and by the National Science Foundation through PLR-1043515. Logistical support for the Antarctic deployment and operations was provided by the NSF through the U.S. Antarctic Program.



Additional Slides

Cryostat Temperature Stages

Temperature Stages:

Vacuum Vessel (VV): **300K**

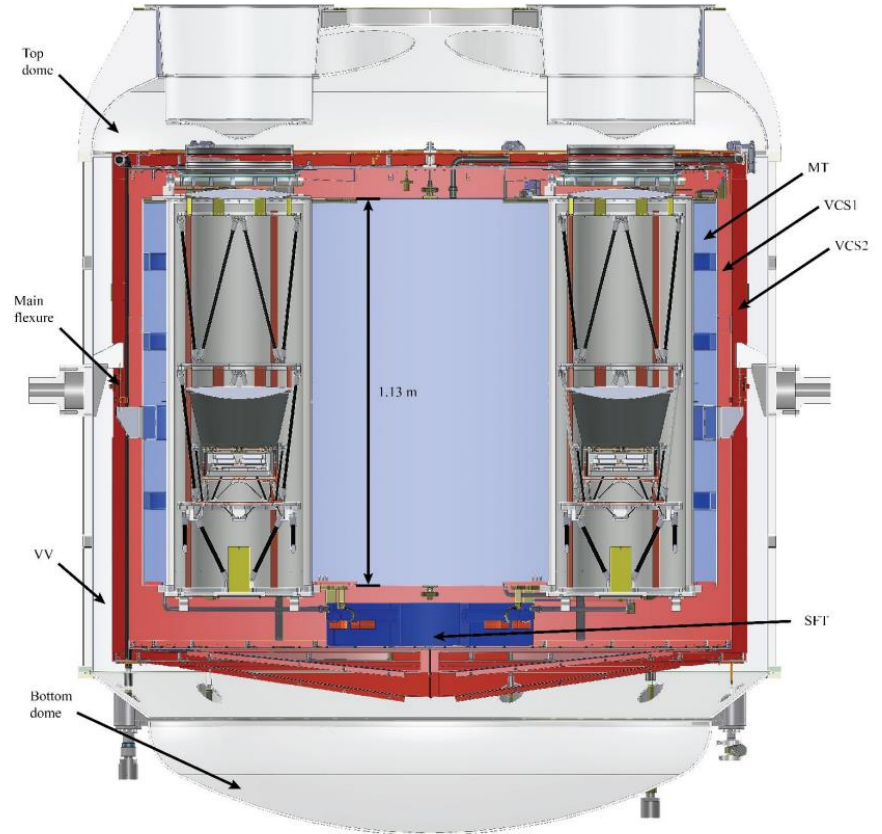
Vapor-Cooled Shield #2 (VCS2): **150K**

Vapor-Cooled Shield #1 (VCS1): **35K**

Liquid Helium Main Tank (MT): **4K**

Super-Fluid Tank (SFT): **2K**

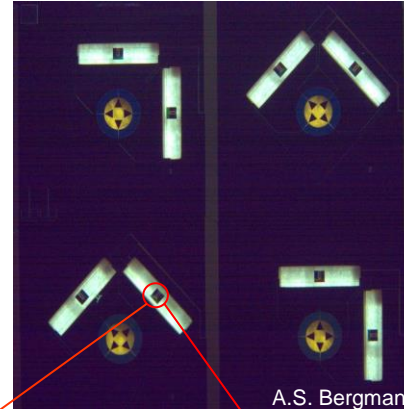
Cold Point of the Helium-3 Fridges: **300mK**



280 GHz Detectors

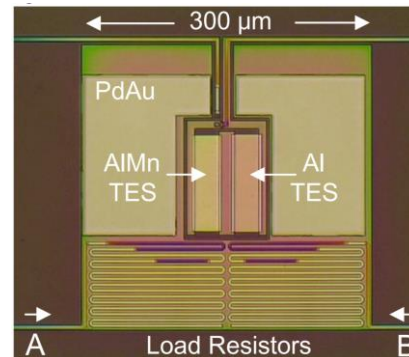
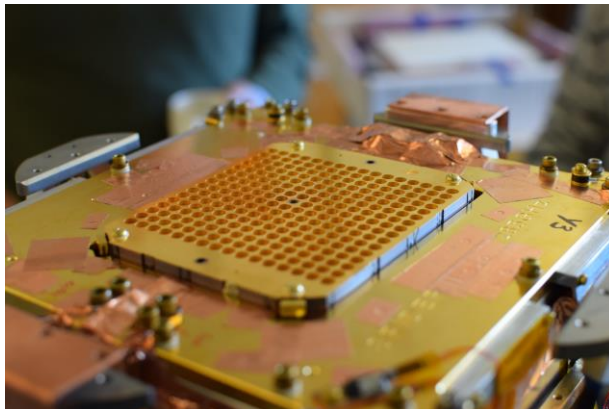
*E. Shaw+ Proc. SPIE (2020).
Bergman+ JLTP (2018)
Hubmayr+ Proc. SPIE (2016)*

- 512 feedhorn-OMT coupled transition-edge sensors (TESs) (*NIST design and fab*)
- Simultaneous coverage of Stokes Q and U polarization
- Dual TES design for easier lab characterization.
- Time-division SQUID multiplexer detector readout (*NIST, UBC*)



A.S. Bergman

NIST

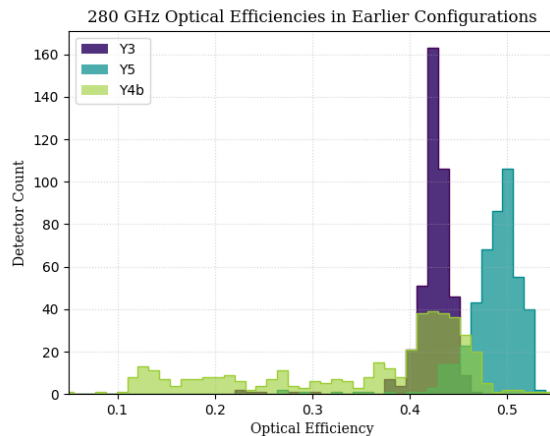
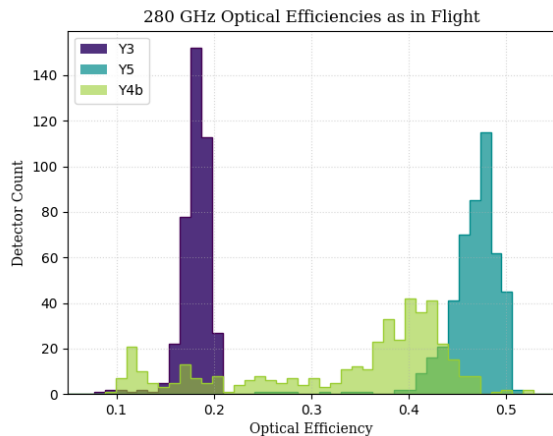
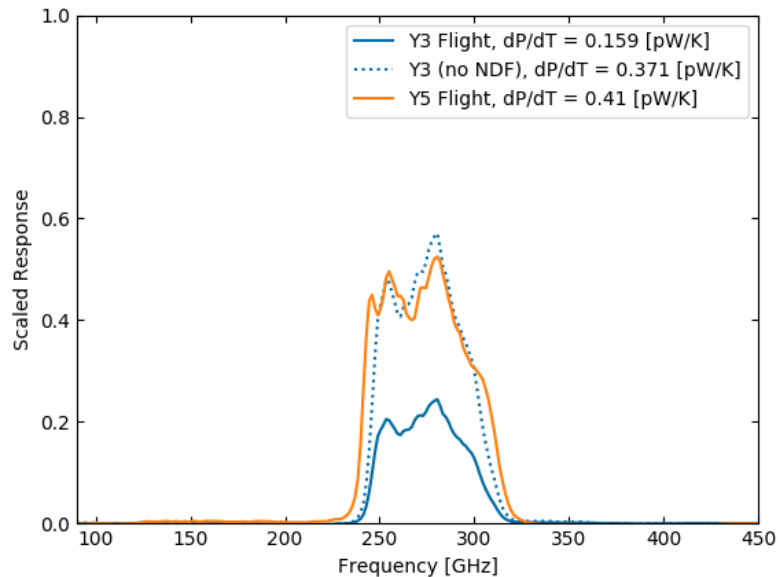


Hubmayr et al. Proc SPIE 1606.09396



280 GHz Spectral Response

- Average FTS spectral response, scaled to match detector responsivity



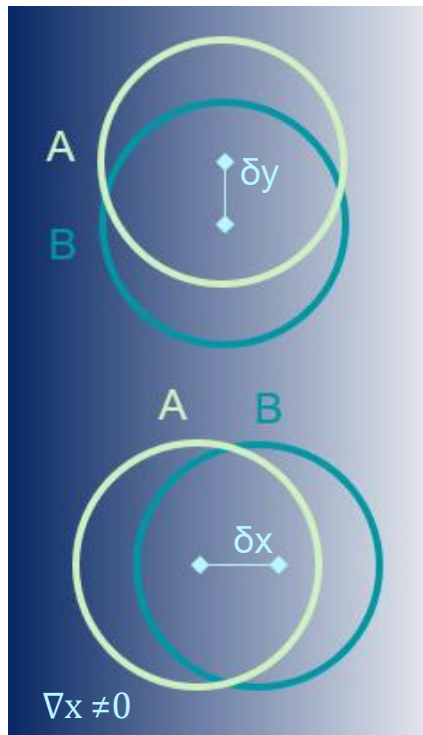
E. Shaw Thesis

Spider 1 Detector Performance

- **Exceptionally low internal loading**
 - **95 GHz:** ≤ 0.25 pW total absorbed power
 - **150 GHz:** ≤ 0.35 pW total absorbed power

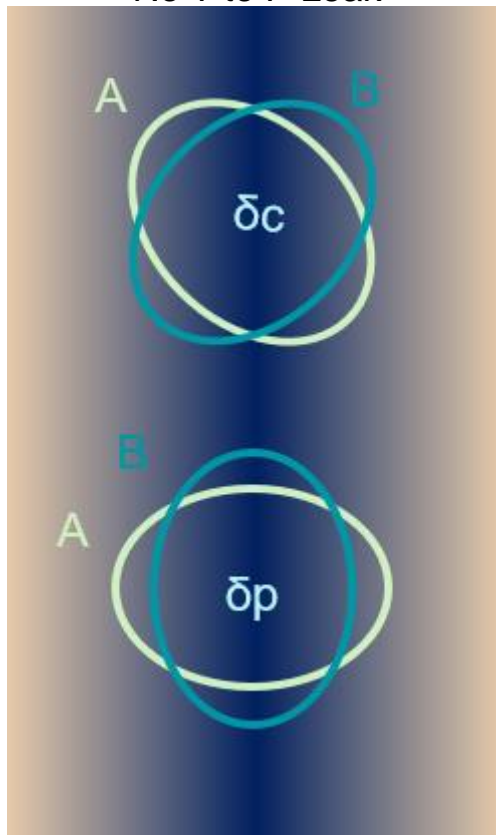
Band	Center [GHz]	Width [%]	FWHM [arcmin]	# Det. Used	NET_{tot} [$\mu\text{K}\sqrt{\text{s}}$]	Data Used [days]	Map Depth [$\mu\text{K} \cdot \text{arcmin}$]
95 GHz	94.7	26.4	41.4	675	7.1	6.5	22.5
150 GHz	151.0	25.7	28.8	815	6.0	5.6	20.4

No T to P Leak



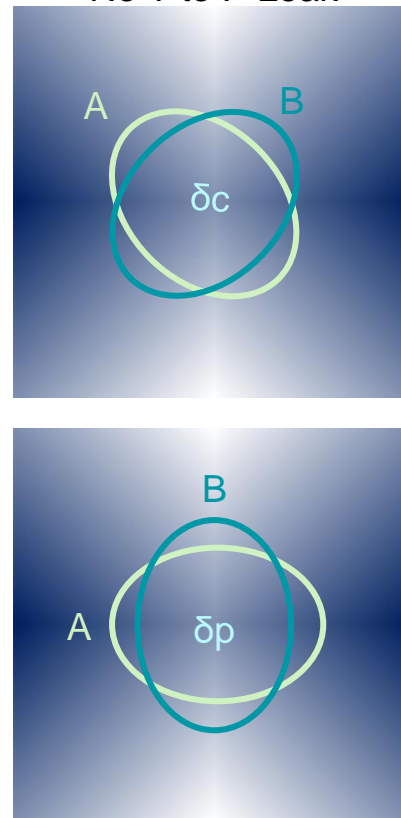
Leaks T to P

No T to P Leak



Leaks T to P

No T to P Leak



Leaks T to P